

Two photon conditional phase gate based on Rydberg slow light polaritons

Przemyslaw Bienias

Joint Quantum Institute, NIST/University of Maryland, College Park,
Maryland 20742, USA
Joint Center for Quantum Information and Computer Science, NIST/University
of Maryland, College Park, Maryland 20742, USA
Institute for Theoretical Physics III, University of Stuttgart, Germany
E-mail: bienias@umd.edu

Hans Peter Büchler

Institute for Theoretical Physics III and Center for Integrated Quantum Science
and Technology, University of Stuttgart, 70550 Stuttgart, Germany

Abstract. We analyze the fidelity of a deterministic quantum phase gate for two photons counterpropagating as polaritons through a cloud of Rydberg atoms under the condition of electromagnetically induced transparency (EIT). We provide analytical results for the phase shift of the quantum gate, and provide an estimation for all processes leading to a reduction to the gate fidelity. Especially, the influence of losses from the intermediate level, dispersion of the photon wave packet, scattering into additional polariton channels, finite lifetime of the Rydberg state, as well as effects of transverse size of the wave packets are accounted for. We show that the flatness of the effective interaction, caused by the blockade phenomena, suppresses the corrections due to the finite transversal size. This is a strength of Rydberg-EIT setup compared to other approaches. Finally, we provide the experimental requirements for the realization of a high fidelity quantum phase gate using Rydberg polaritons.

PACS numbers: 34.20.C, 32.80.Ee, 42.50.Gy, 42.50.Nn

Introduction — Photons interact extremely weakly with each other, propagate with the speed of light and provide a high bandwidth. These three features make photons an excellent carrier of information. However, for applications in quantum information processing [1], interactions on the level of single quanta are necessary. Such interactions can be achieved by coupling photons to matter [2, 3, 4, 5, 6]. Especially, Rydberg-EIT (rEIT) has emerged a promising approach [7, 8, 9, 10, 11, 12, 13] visible in great experimental [14, 4, 15, 16, 17, 18, 19, 20, 21, 22, 23, 24, 25, 26, 27, 28] and theoretical [29, 30, 30, 31, 32, 33, 34, 35, 36, 37, 38, 39, 40, 41, 42, 43, 44, 45, 46, 47, 48, 49, 50, 51, 52, 53, 54, 55] progress. A photonic quantum phase gate using Rydberg-EIT in a counter-propagating setup was first discussed by Friedler et al. [56] and an extended description was shown by Gorshkov et al. [30]. However, a study including all effects that decrease the fidelity of the phase gate, as well as, a discussion of a specific microscopic setup is still missing. Here, we attempt to fill this gap by analyzing within a microscopic description the different source for a reduction in gate fidelity in a realistic setup.

Recently, a few alternative approaches for a quantum phase gate have emerged [57, 58], which were motivated (at least partially) by the belief that the link between propagation and interaction [59, 60] precludes high-fidelity gates whenever a cross-phase modulation (XPM) on a single photon level is used. However, for the Rydberg-EIT setup the interaction between Rydberg polaritons has a finite range and Rydberg polaritons acquire an effective mass in addition to the linear slow light velocity, and therefore the proposed no-go theorems [59, 60, 61] do not apply [55].

The effective interaction between Rydberg polaritons has an important feature, namely that the interaction potential is flat [40] for distances smaller than interaction range (called blockade radius which is on the order of $10\mu\text{m}$). This feature could in principle enable a phase gate in a copropagating configuration, which in general is characterized by longer interaction times and therefore could enable greater phase shifts. However, the condition of a homogeneous phase shift requires compression of photons to the size of the blockade radius. This violates the conditions for neglecting the mass term which depicts the quadratic corrections to the polaritonic dispersion relation. In turn, adding the mass term leads to strong mode distortion pre-

cluding the realization of a photonic quantum gate in a copropagating setup. Thus, the phase gate might be possible only if photons pass each other by for example being counter-propagating [62, 63, 56, 64] or having different group velocities [65].

In this manuscript, we study a quantum phase gate for photons in a counter-propagating setup using the microscopic theory describing the Rydberg slow light polaritons. The main focus is on providing an analytical expression for the imprinted phase, as well as a detailed analysis of different sources for a reduction in the gate fidelity. In addition to standard effects such as losses from the intermediate state and Rydberg levels, we also include propagation effects such a dispersion of the wave packet and energy dependence of the phase shift, as well as the influence of scattering into different polariton channels. Note, that our approach does not rely on semiclassical approximations recently applied [36], but is based on the full microscopic quantum description for two photons. We provide the experimental requirements for the realization of a high fidelity quantum phase gate using Rydberg polaritons.

General concept— The qubit is encoded in the polarization of the photons, and the excitation into the Rydberg levels depends on this polarization [20]. Then, photons within the Rydberg medium are propagating as Rydberg polaritons, see Fig. 1. After passing each other, they pick-up the phase shift due to the strong interaction between Rydberg atoms, leading to the interaction induced phase shift only between photons having a specific polarization. We will discuss a microscopic setup in detail at the end of the manuscript. We define the fidelity F and phase shift ϕ of the gate using the overlap between the two-photon wave-functions with $(\mathcal{E}\mathcal{E})$ and without $(\mathcal{E}\mathcal{E}^{V=0})$ the interaction V between the polaritons:

$$\sqrt{F}e^{i\phi} = \langle \mathcal{E}\mathcal{E}^{V=0} | \mathcal{E}\mathcal{E} \rangle. \quad (1)$$

Our definition of the fidelity includes all detrimental effects and is more restrictive than commonly used [66, 36] conditional-fidelity in which two output states are normalized [67],

$$\sqrt{F_{\text{cond}}}e^{i\phi} = \langle \mathcal{E}\mathcal{E}^{V=0} | \mathcal{E}\mathcal{E} \rangle / \langle \mathcal{E}\mathcal{E}^{V=0} | \mathcal{E}\mathcal{E}^{V=0} \rangle. \quad (2)$$

We will identify the leading contributions to the fidelity by different physical phenomena

$$F = (\beta_\gamma \beta_{\text{sc}} \beta_{\text{wp}} \beta_{\text{at}} \beta_{\text{Ry}} \beta_{\text{tr}})^2. \quad (3)$$

Here,

- β_γ accounts for the spontaneous emission from the

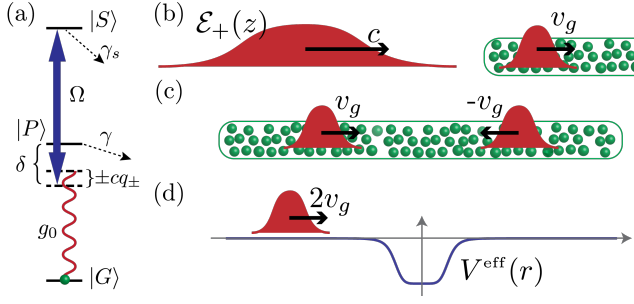


Figure 1. (a) The probe field couples the atomic ground state $|G\rangle$ to the p -level $|P\rangle$ with the single-particle coupling strength g_0 , while a strong coupling laser drives the transition between the p -level and the Rydberg state $|S\rangle$ with Rabi frequency 2Ω and detuning δ . Furthermore, γ denotes the halfwidth of the p -state and γ_s the halfwidth of the s -state. The single-particle coupling g_0 is related to the collective coupling $g = \sqrt{n_{\text{at}}}g_0$ with n_{at} the particle density. Note that the kinetic energy of the photons $\pm\hbar c q_{\pm}$ accounts for the difference to the EIT condition, and in the position space takes the form $\mp i\hbar c \partial_z$. (b) Photon entering the EIT medium is compressed by factor v_g/c . For pulses shorter than the length of the medium, photons enter the medium without backscattering and losses because interaction between polaritons can be neglected and spatial density variations are smooth on the scales of photonic wavelength. (c) Two counter-propagating polaritons inside the medium. (d) In the center of mass frame, the problem simplifies to the scattering on the effective potential $V^{\text{eff}}(r)$, which leads to the interaction induced phase shift.

intermediate p -level caused by the interaction,

- β_{sc} accounts for scattering into additional polariton channels,
- β_{wp} includes the impact of the finite length of the wave-packets on (a) the losses from p -state during propagation and (b) the inhomogeneous interaction-induced phase-shift
- β_{at} describes the distortion of the phase shift due to spatially varying atomic density,
- β_{Ry} denotes losses due to the finite lifetime of the Rydberg state, whereas
- β_{tr} depicts finite beam waist effects leading to scattering of photons to other transversal photonic modes.

At this point it is worth mentioning the family of phase-gate schemes in which at least one photon [58, 57, 27, 68, 69, 70] is stored as a collective atomic excitation. This type of schemes is superior compared to counter-propagating scheme when it comes to the β_{sc} and β_{wp} in equation Eq. 3. However, such quantum gates suffer from an additional factor decreasing the fidelity, which accounts for the finite storage and retrieval probability of the photons; for an efficient storage and retrieval [71, 72, 73], such schemes can be preferable in some circumstances.

Propagation inside the medium: First, we consider photons characterized by a single transverse mode propagating through an atomic ensemble [74] where

the atomic ground state is coupled to a Rydberg s -state via an intermediate short-lived p -state, see Fig. 1(a). We introduce the electric field operators $\hat{\mathcal{E}}_+^\dagger(z)$ and $\hat{\mathcal{E}}_-^\dagger(z)$ creating at position z photons propagating to the right and left, respectively. For the atomic density much higher than the photonic density, the excitations of atoms generated by right- and left- moving photons into s -level and p -level are well-described by the bosonic field operators $\hat{\mathcal{S}}_\pm^\dagger(z)$ and $\hat{\mathcal{P}}_\pm^\dagger(z)$, respectively [30][‡]. Then, we obtain the non-interacting part of the microscopic Hamiltonian [30, 40], i.e., $H_+ + H_-$, under the rotating-wave approximation within the rotating frame, where

$$H_\pm = \hbar \int dz \begin{pmatrix} \hat{\mathcal{E}}_\pm \\ \hat{\mathcal{P}}_\pm \\ \hat{\mathcal{S}}_\pm \end{pmatrix}^\dagger \begin{pmatrix} \mp i\hbar c \partial_z & g & 0 \\ g & \Delta & \Omega \\ 0 & \Omega & 0 \end{pmatrix} \begin{pmatrix} \hat{\mathcal{E}}_\pm \\ \hat{\mathcal{P}}_\pm \\ \hat{\mathcal{S}}_\pm \end{pmatrix}. \quad (4)$$

Here, g denotes the collective coupling of the photons to the matter via the excitation of ground state atoms into the p -level, while 2Ω denotes the Rabi frequency of the control field between the p -level and the Rydberg state, Fig. 1. Note that the kinetic energy of the photons $\mp i\hbar c \partial_z$ accounts for the deviation from the EIT condition. We introduced the complex detuning $\Delta = \delta - i\gamma$, which accounts for the detuning δ of the control field and the decay rate 2γ from the p -level. Since we are interested in two counter-propagating polaritons, the interaction between the Rydberg levels is described by

$$H_{\text{rr}} = \int dz \int dz' V(z - z') \hat{\mathcal{S}}_+^\dagger(z) \hat{\mathcal{S}}_-^\dagger(z') \hat{\mathcal{S}}_-(z') \hat{\mathcal{S}}_+(z).$$

The full scattering of the two photons inside the media is well accounted for by the T -matrix. As the interaction acts only between Rydberg states, it is sufficient to study the T -matrix for the Rydberg states alone, which is denoted as $T_{kk'}(K, \omega)$. Here, $\hbar K = \hbar(q_+ + q_-)$ denotes the center of mass momentum and $\hbar\omega$ the total energy, while $\hbar k'$ ($\hbar k$) is the incoming (outgoing) relative momentum. Note, that the total energy $\hbar\omega$ as well as the center of mass momentum $\hbar K$ are conserved in our system. The resummation of all ladder diagrams [40] leads to the integral equation

$$T_{kk'}(K, \omega) = V_{k-k'} + \int \frac{dq}{2\pi} V_{k-q} \chi_q(K, \omega) T_{qk'}(K, \omega). \quad (5)$$

The full pair propagator of two counter-propagating polaritons and its overlap with the Rydberg state takes the form

$$\chi_q = \bar{\chi} + \frac{\alpha_D}{\hbar k_D(K, \omega) - \hbar q + i0^+} + \sum_{j=1}^4 \frac{\alpha_j}{\hbar k_j(K, \omega) - \hbar q + i0^+}. \quad (6)$$

[‡] For example, slowly varying field operators $\hat{\mathcal{P}}_\pm$ are defined via $\hat{\mathcal{P}}_\pm(z) = \hat{\mathcal{P}}_\pm(z) e^{\mp i k_p z + i \omega_p t}$ where $\hat{\mathcal{P}}$ is the field operator before going to the rotating frame whereas $\omega_p = c k_p$ is the carrier frequency of the probe field.

and is shown in Fig. 2(b). Here, $\bar{\chi}$ accounts for the saturation of the pair propagation at large relative momenta $\hbar q \rightarrow \pm\infty$, and takes in the relevant regime $\Omega \ll |\Delta|$ the form

$$\bar{\chi}(\omega) = \frac{\Delta}{2\hbar\Omega^2} \frac{1}{1 + \frac{\omega\Delta}{2\Omega^2}}. \quad (7)$$

The second term in Eq. 6 is the pole structure for the propagation of the two incoming dark-state polaritons. The general expression of α_D and k_D are complicated, therefore we provide below its analytical form only in the experimentally relevant regimes. The last sum accounts for the resonant scattering of the two incoming dark polaritons into four outgoing channels containing at least one bright polariton, see Fig. 2. Note that in contrast to the copropagating equation, where the massive-like behavior can be neglected only in certain regimes [55], here, the kinetic part is always linear in the relative momentum. Thus, the large phase shift is possible without a drop of the fidelity caused by the distortion of the wave-packet shape, as well as, we can derive analytical results.

In the following, we derive the scattering phase shift during the collision of two dark polaritons. The first important step is to notice the relation between the scattering wave function $\psi_k^{ss}(r)$ describing the amplitude to find two Rydberg excitations for the incoming relative momentum k' ,

$$\psi_k^{ss}(r) = \frac{1}{V(r)} \int \frac{dk}{2\pi} e^{ikr} T_{kk'} \equiv \frac{T_{k'}(r)}{V(r)}, \quad (8)$$

which follows from the close analogy of Eq. (5) to the Lippmann-Schwinger equation in the scattering theory [40]. Note that for photons of interest close to EIT resonance (i.e., $|K|, |k'| \ll g^2/|\delta|c$) and for $|r| \gg \xi$, we have $\psi_k^{ss}(r) = \frac{g^2}{\Omega^2} \mathcal{E}\mathcal{E}_{k'}(r)$. In the next step, we absorb the saturation $\bar{\chi}$ by introducing the effective interaction potential [40]

$$V^{\text{eff}}(r) = \frac{V(r)}{1 - \bar{\chi}(\omega)V(r)}. \quad (9)$$

The effective interaction potential saturates for short distances at $-1/\bar{\chi}$ and is characterized by the blockade radius ξ , which for a van der Waals interaction takes the form $\xi = (|C_6\Delta/2\hbar\Omega^2|)^{1/6}$. Then, Eq. (5) for the T -matrix simplifies to

$$T_{kk'} = V_{k-k'}^{\text{eff}} + \int \frac{dq}{2\pi} V_{k-q}^{\text{eff}} [\chi_q - \bar{\chi}] T_{qk'} \quad (10)$$

and includes the contribution from all different poles in the two-particle propagator.

Finally, we focus on the experimentally relevant regime described by slow light polaritons $g \gg \Omega$ with large single photon detuning $|\Delta| \gg \Omega$. Then, the last term in Eq. (6) describing scattering into a bright polaritons is strongly suppressed for small energies $|\omega| \leq 2\Omega^2/|\Delta|$; the influence of these additional

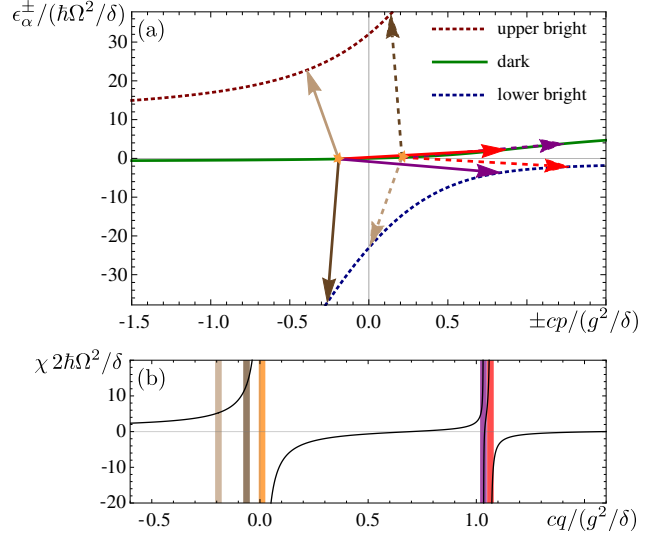


Figure 2. (a) Dispersion relations for the right- and left-propagating fields are shown using the property that $\epsilon_{\alpha}^{-}(-p) = \epsilon_{\alpha}^{+}(p)$, see Eq. 4, and therefore the curves overlap. For each direction of propagation, three noninteracting polariton branches exist. Two dark state polaritons (denoted by stars) can scatter into four channels, each represented by the different colour of arrows. Solid lines correspond to right-propagating and dashed lines to left-propagating polaritons. Note that the total momentum $\hbar K$ and energy $\hbar\omega$ are conserved during the scattering process. Strongly suppressed losses into two bright polaritons are described by light and dark brown arrows. Crucial losses into bright-dark polariton pair are depicted by red and purple arrows. (b) Full pair propagator χ in the function of relative momentum $\hbar c q$. Vertical lines depict relative resonant momenta with colors corresponding to colors of arrows and stars from figure (a). Note that both light and dark brown resonances are so narrow that cannot be resolved in the plot, and that resonance for pair of dark polaritons (orange) is much wider than purple and red resonances. All results are presented for $g = 3\delta$, $\delta = 3\Omega$, $\gamma = 0$, $\omega = 0.1 \times 2\Omega^2/\delta$, $K = -0.4 g^2/\delta c$.

processes on the gate fidelity can be discussed within perturbation theory, see below. In the leading order, we can therefore neglect these terms and study the T -matrix with the dominant pole for the propagation of the dark polaritons alone. Within this regime, we obtain expressions in function of K and ω

$$\alpha_D(K, \omega) = \frac{g^2}{\Omega^2 c} \left(\frac{1}{2\sqrt{\left(\frac{c\Delta K}{g^2}\right)^2 \left(\frac{\Delta\omega}{2\Omega^2} + 1\right)^2 + 1}} + \frac{1}{2} \right),$$

$$k_D(K, \omega) = \frac{g^2}{2\Delta c} \frac{1 + \frac{\Delta\omega}{\Omega^2} - \sqrt{1 + \left(\frac{c\Delta K}{g^2}\right)^2 \left(\frac{\Delta\omega}{2\Omega^2} + 1\right)^2}}{1 + \Delta\omega/(2\Omega^2)}.$$

Furthermore, we are interested in scattering processes where the incoming momentum is on-shell and describes two dark polaritons, thus, the incoming momentum $\hbar k'$ reduces to $\hbar k_D$ with conserved energy $\hbar\omega$ and center of mass momentum $\hbar K$. Then, the equation for the T -matrix can be analytically solved

and takes the form

$$T_{k_D}(r) = V^{\text{eff}}(r) e^{ik_D r} \exp \left[-i \frac{\alpha_D}{\hbar} \int_{-\infty}^r dz V^{\text{eff}}(z) \right]. \quad (11)$$

With the relation (8) between the scattering wave function and the T -matrix, the final result for the phase shift due to the collision of the two dark polaritons takes the form

$$\begin{aligned} \psi_{k_D}^{ss}(r) &= \frac{1}{1 - \bar{\chi} V(r)} e^{ik_D r} \exp \left[-i \frac{\alpha_D}{\hbar} \int_{-\infty}^r dz V^{\text{eff}}(z) \right] \\ &= \begin{cases} e^{ik_D r} & r \rightarrow -\infty \\ e^{i\varphi} e^{ik_D r} & r \rightarrow \infty \end{cases} \end{aligned} \quad (12)$$

with the phase shift

$$\varphi = -\frac{\alpha_D}{\hbar} \int_{-\infty}^{\infty} dz V^{\text{eff}}(z). \quad (13)$$

Note, that the wave function is strongly suppressed within the blockade region $|r| < \xi$ due to the blockade phenomena quenching two Rydberg excitations at short distances. In the presented leading order, the scattering into additional channels is suppressed and therefore we obtain only a phase shift. The phase shift contains an imaginary part accounting for the losses during the scattering process by spontaneous emission from the intermediate p -level. Performing the remaining integration for a microscopic van der Waals interaction, the phase reduces to

$$\varphi(K, \omega) = \alpha_D(K, \omega) \frac{2\pi g^2 \xi (-\text{sgn}[C_6] \Delta)^{1/6}}{3c|\Delta|^{1/6} \Delta \left(\frac{\Delta \omega}{2\Omega^2} + 1 \right)^{7/6}}. \quad (14)$$

Note, that the phase still depends on the center of mass momentum and the total energy, and therefore, we expect a weakly inhomogeneous phase shift for a wave packet. The leading contribution is determined on the two-photon resonance, i.e., $\omega = 0$ and $K = 0$, where the solution agrees with [75]. For $\gamma \ll |\delta|$ the exponent φ simplifies to

$$\phi + i\eta = \frac{2\pi g^2 \xi}{3\delta c} \left(1 + i \frac{5}{6} \frac{\gamma}{\delta} \right), \quad (15)$$

where ϕ describes the coherent phase shift and can be expressed using optical depth κ_ξ per blockade radius, $\phi = (\pi/3) \kappa_\xi \gamma / \delta$. In turn η denotes the losses via spontaneous emission from the p -level and therefore provides a reduction of the outgoing wave function, i.e.,

$$\beta_\gamma^2 = e^{-2\eta} \approx 1 - 2\eta. \quad (16)$$

The β_γ is the main contribution to the reduction of the gate fidelity, and it requires the far detuned regime $|\delta| \gg \gamma$ in combination with large optical depth per blockade radius.

Scattering into additional open channels—Next, we continue with a detailed analysis of all additional contributions leading to a reduction of the gate fidelity. We start with the study of the influence of the

additional poles in the two polariton propagator χ , see Fig. 2. These poles describe additional open channels characterized by the relative momenta k_j . Therefore, the interaction between the polaritons leads to scattering of the incoming dark polaritons into these open channels. Consequently, the outgoing wave function takes the form

$$\psi_{k_D}^{ss}(r) = \beta_{sc} e^{i\varphi} e^{ik_D r} + \sum_{j=1}^4 \epsilon_j e^{ik_j r}, \quad (17)$$

with $|\beta_{sc}|^2$ a reduced probability to remain in the dark polariton state, and $|\epsilon_j|^2$ a probability to be in the other channel. The analysis can be performed straightforwardly in lowest order perturbation theory in α_j/α_D . Then, the correction δT to the T -matrix is determined by the equation

$$\begin{aligned} \delta T_{k_D}(r) &= -\frac{i\alpha_D}{\hbar} V^{\text{eff}}(r) e^{ik_D r} \int_{-\infty}^r dz e^{-ik_D z} \delta T_{k_D}(z) \\ &\quad - \sum_{j=1}^4 \frac{i\alpha_j}{\hbar} V^{\text{eff}}(r) \int_{-\infty}^r dz e^{ik_j(r-z)} T_{k_D}(z). \end{aligned} \quad (18)$$

The general solution takes the form

$$\begin{aligned} \delta T_{k_D}(r) &= \sum_{j=1}^4 \frac{\alpha_j}{\alpha_D} \left\{ e^{ik_j r} V^{\text{eff}}(r) \int_{-\infty}^r dz e^{i(k_D - k_j)z} \partial_z e^{i\theta(z)} \right. \\ &\quad \left. - T_{k_D}(r) \int_{-\infty}^r dz \int_{-\infty}^z dy e^{i(k_j - k_D)(z-y)} \partial_z e^{-i\theta(z)} \partial_y e^{i\theta(y)} \right\}, \end{aligned}$$

where $\theta(z) = -\alpha_D \int_{-\infty}^z dy V^{\text{eff}}(y)/\hbar$. The first term describes the weight in the additional open channels, i.e.,

$$\epsilon_j = \frac{\alpha_j}{\alpha_D} \int_{-\infty}^{\infty} dz e^{i(k_D - k_j)z} \partial_z e^{i\theta(z)} \quad (19)$$

whereas the second term accounts for the reduction of the outgoing dark polariton state, and can be written in leading order α_j/α_D as

$$1 - |\beta_{sc}|^2 = 2 \sum_{j=1}^4 \frac{\alpha_j}{\alpha_D} \left| \int_{-\infty}^r dz \int_{-\infty}^z dy e^{i(k_j - k_D)(z-y)} \partial_z e^{-i\theta(z)} \partial_y e^{i\theta(y)} \right|.$$

In order to estimate the value of the suppression, it is sufficient to focus on the resonant regime with $\omega = 0$ and $K = 0$. Then, the values of momenta k_j and the weight of the residues α_j take a simple analytical form. Specifically, in the experimentally relevant regime with $\Omega \ll g$, we find that the poles group into pairs of equal weight

$$k_1 = k_2 = \frac{g^2}{\Delta c}, \quad \alpha_1 = \alpha_2 = \frac{g^2 + \Delta^2}{4\Delta^2 c}, \quad (20)$$

$$k_3 = k_4 = -\frac{\Delta}{c}, \quad \alpha_3 = \alpha_4 = \frac{g^2 \Omega^4}{4(g^2 + \Delta^2)^3 c}. \quad (21)$$

The first two poles describe excitations at high relative momentum, whereas the second pair of poles at low

relative momenta which is always strongly suppressed for slow light polaritons, see Fig. 2. Therefore, the reduction due to the scattering into the additional open channels can be estimated to satisfy the inequality

$$|\beta_{\text{sc}}|^2 \gtrsim 1 - \phi^2 |2\alpha_1/\alpha_D| = 1 - \phi^2 \frac{\Omega^2}{|\Delta|^2} \frac{|\Delta|^2 + g^2}{2g^2}. \quad (22)$$

This term is suppressed for $\Omega \ll |\Delta|$, which provides an additional constraint on the experimental parameters.

Wave packet propagation— The next step is to study the influence of realistic wave packets onto the gate fidelity. There are two different contributions: First one is a distortion of the wave packet due to the non-linear corrections to the dispersion relation of the dark polariton, which is also present for noninteracting polaritons. Second contributions comes from the dependence of phase factor φ on K and ω leading to the longitudinally inhomogeneous phase shift for wave packets. In the following, both phenomena will be discussed in detail.

The right and left moving photonic wave packets inside the homogeneous atomic media are described by the slowly varying envelope for the electric field,

$$\mathcal{E}_{\pm}(z, t) = \int \frac{d\nu}{2\pi} \mathcal{E}_{\pm}(\nu) \exp[\pm i p(\nu)(z - L_{\pm}) - i \nu t]. \quad (23)$$

Here, $\mathcal{E}_{\pm}(L_{\pm}, t)$ describes the electric field of the incoming photonic wave packet at the boundary of the atomic media with $L = L_+ - L_-$ the length of the media, see Fig. 1. In addition, the momentum $\hbar p(\nu)$ of a polariton is related to frequency ν by the dispersion relation for dark polaritons. The momentum exhibits the general form

$$p(\nu) = \nu \frac{g^2 + \Omega^2 + \Delta\nu - \nu^2}{c(\Omega^2 + \Delta\nu - \nu^2)} \approx \frac{\nu}{v_g} - \frac{\hbar\nu^2}{2m\nu v_g^3}, \quad (24)$$

which in the experimentally relevant regime close to the EIT resonance is well described by the slow light velocity $v_g = c\Omega^2/g^2$ and the effective mass $m = \hbar g^4/(2c^2\Delta\Omega^2)$. The mass leads to a wave packet dispersion as well as losses from the intermediate p -level due to the imaginary part of the mass. Note that even though it looks as if the mass term contributes to the dynamics of the pair of polaritons, the physics is more subtle. Namely, in Eq. 6 we showed that two-photon-dynamics for conserved K, ω has a linear dependence on the relative momentum [which allows simple analytical solution, Eq. 11]. However, a conserved relative momentum k_D is a function of K, ω and m which corresponds to Eq. 24 which we analyze here.

The probability for the polariton to pass through the media is given by

$$P_{\pm} = \int \frac{d\nu}{2\pi} |\mathcal{E}_{\pm}(\nu)|^2 e^{-2p''(\nu)L}, \quad (25)$$

where $p''(\nu)$ denotes the imaginary part of $p(\nu)$. Therefore, the dipolar interaction between two polaritons leads to two effects: first, a weak shift for the scattering phase $\Delta\phi$ due to the averaging over different energy and momentum states, secondly, a reduction in the gate fidelity β_{wp} . Both quantities are determined by the equation

$$\beta_{\text{wp}} e^{i\Delta\phi} = \int \frac{d\nu_1 d\nu_2}{(2\pi)^2} |\mathcal{E}_+(\nu_1) \mathcal{E}_-(\nu_2)|^2 e^{-2L[p''(\nu_1) + p''(\nu_2)]} \times \exp[i\varphi(K, \omega) - i\phi + \eta]. \quad (26)$$

It is important that $\varphi(K, \omega)$ depends on the total energy $\hbar\omega = \hbar\nu_1 + \hbar\nu_2$ and the center of mass momentum $\hbar K = \hbar p(\nu_1) - \hbar p(\nu_2)$.

In order to illustrate the phenomena of the wave packet propagation, we focus on a Gaussian incoming wave packet

$$\mathcal{E}_{\pm}(\nu) = \frac{\exp[-\nu^2/2\sigma^2]}{(\pi\sigma^2)^{1/4}} \quad (27)$$

with a small bandwidth $\sigma \ll \Omega^2/|\Delta|$. Then, it is sufficient to keep the leading quadratic corrections in ω and K . First, the impact on the fidelity simplifies to

$$\beta_{\text{wp}} = P_+ P_- \exp\left[-\frac{49}{2}\phi^2 \left(\frac{\sigma|\Delta|}{12\Omega^2}\right)^2\right], \quad (28)$$

with

$$P_{\pm} = \exp\left[-2\frac{Lg^2}{\delta c} \left(\frac{\delta\sigma}{\Omega^2}\right)^2 \frac{\gamma}{\delta}\right]. \quad (29)$$

Second, the shift in the coherent phase reduces to

$$\Delta\phi = \frac{19}{2}\phi \left(\frac{\sigma|\Delta|}{12\Omega^2}\right)^2. \quad (30)$$

Impact of atomic distribution— Additional contribution to the fidelity comes from the inhomogeneity of the atomic distribution. To illustrate this effect, we consider Gaussian atomic distribution $n_{\text{at}}(z) = n_0 \exp[-z^2/\mathcal{L}^2]$, where \mathcal{L} characterizes the cloud's length. In the relevant regime of $\xi \ll \mathcal{L}$, the scattering phase shift depends locally on the atomic density at which two polaritons interact with each other. Inside the medium photons are compressed to the size $\sigma_z = c\Omega^2/(g^2\sigma)$, where g in this paragraph denotes the value of collective coupling at the center of the cloud. For short photons $\sigma_z \ll \mathcal{L}$, the corrections to the fidelity and phase shift take the form [67]

$$\beta_{\text{at}} e^{i\Delta\phi_{\text{at}}} = 1 - i\phi \left(\frac{\sigma_z}{2\mathcal{L}}\right)^2 - \frac{3}{2}\phi^2 \left(\frac{\sigma_z}{2\mathcal{L}}\right)^4. \quad (31)$$

This puts additional constraint on the length of the medium: $\mathcal{L} \gg \sigma_z$.

Transversal size of the photons— Two colliding wave-packets in the lowest Laguerre-Gauss mode are described by $\mathcal{E}_{\pm}(z_{\pm}, \mathbf{R}_{\pm}) = \mathcal{E}(z_{\pm})u(\mathbf{R}_{\pm})$ with $u(\mathbf{R}) = \exp[-(x^2 + y^2)/w_0^2] \sqrt{2/\pi}/w_0$ where w_0 is the probe

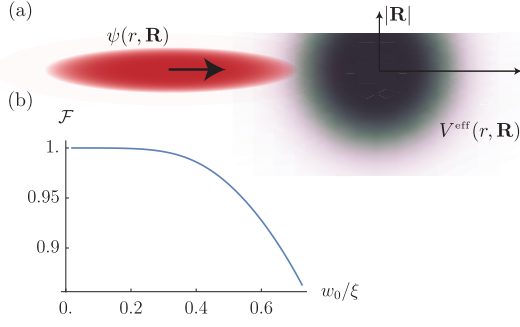


Figure 3. (a) Two-photon wave-function, having finite transverse size, scatters in center-of-mass (i.e., $z_- + z_+ = \text{const.}$ and $\mathbf{R}_+ + \mathbf{R}_- = \text{const.}$) frame on the effective potential $V^{\text{eff}}(r, \mathbf{R})$, where $\mathbf{R} = \mathbf{R}_+ - \mathbf{R}_-$. (b) Fidelity as a function of a transverse width σ_\perp for the phase shift $\phi = \pi/2$: The drop of the fidelity for $w_0/\xi < 0.35$ is negligible. Intuitively, due to the plateauing of V^{eff} , photons experience a homogeneous transversal phase shift.

beam waist. The interaction potential generalized to a quasi-1D geometry depends on the relative transversal distance, $V^{\text{eff}}(r, \mathbf{R}) = V(\mathbf{r})/(1 - \bar{\chi}(\omega)V(\mathbf{r}))$, [67]. For beam waist comparable to the blockade radius, this leads to the transversely inhomogeneous phase shift [56, 76, 44]. To estimate the correction to the fidelity, we neglect transversal part of the photonic paraxial wave equation [67], which leads to β_{tr} being equal to

$$\left| \int d\mathbf{R}_+ d\mathbf{R}_- |u(\mathbf{R}_+)u(\mathbf{R}_-)|^2 \exp[i\varphi(|\mathbf{R}_+ - \mathbf{R}_-|, \xi)] \right|.$$

From β_{tr} in the limit of $\gamma/\delta \rightarrow 0$ [Fig. 3(b)] we see that the drop of fidelity can be neglected for $w_0/\xi \lesssim 0.35$, which for exemplary experimental parameters, $w_0 = 4.2 \mu\text{m}$, $|nS\rangle = |100S\rangle$, $\Omega = \gamma$, and $\delta = 5\gamma$, gives $w_0/\xi = 0.17$. Intuitively, the reason for this behavior is that polaritons interact via $V^{\text{eff}}(\mathbf{r})$ which is nearly constant for the distances shorter than the blockade radius. It is an important feature of Rydberg polaritons resulting in the phase shift being nearly homogeneous also in the transverse direction. Note that this feature is no longer present in the proposals based on the pulses propagating in two parallel but spatially-separated photonic modes [36] and should be carefully taken into account.

Rydberg lifetime—can be estimated using delay time L/v_g the polariton spends inside the medium during which it is primarily of Rydberg character, which leads to $\beta_{\text{Ry}} = \exp[-4\gamma_s \frac{L}{v_g}]$.

Experimental realization—Two-qubit conditional quantum phase gate (QPG) [77, 2, 78] is universal because combined with rotations of individual qubits enables any quantum computation. The QPG transformation reads

$$|b, j\rangle \rightarrow \exp[i\phi \delta_{b,\downarrow} \delta_{j,\downarrow}] |b, j\rangle, \quad (32)$$

where $|b\rangle, |j\rangle$ depict basis states $|\uparrow\rangle$ and $|\downarrow\rangle$ of the two qubits of interest and $\delta_{b,\downarrow} \delta_{j,\downarrow}$ are standard Kronecker

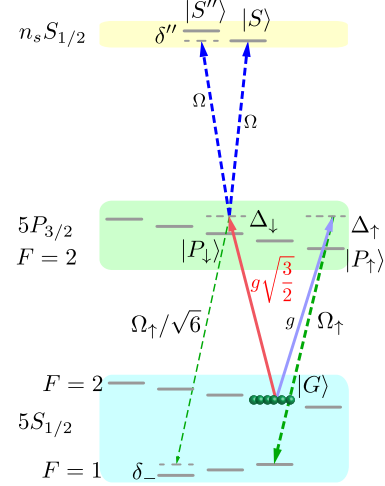


Figure 4. Atomic scheme. Assuming repulsive vdW interactions and choosing $\delta'' \gg \Omega^2 / |\Delta_\uparrow|$ as well as $\delta_\downarrow < 0$ (where $\Delta_\downarrow = \delta_\downarrow - i\gamma$), we avoid Raman resonance for $|S\rangle$ and $|S''\rangle$, as well as, can neglect coupling to $|S''\rangle$ at all. See main text for additional description.

symbols. It is important to stress that QPG leaves basis states unchanged except a homogeneous phase shift ϕ when both are in $|\downarrow\rangle$ state. In order to implement the gate, it is important that both states $|\uparrow\rangle$ and $|\downarrow\rangle$ acquire the same time delay inside the medium, but only the state $|\downarrow\rangle$ becomes a Rydberg polariton. In Fig. 4, we show the atomic scheme which satisfies this condition. As a ground state we take $|g\rangle = |5^2S_{1/2}, F=2, m_F=1\rangle$ from which we couple with σ_+ polarized photons to $|p_\uparrow\rangle = |5^2P_{3/2}, F=2, m_F=2\rangle$, and with σ_- -polarized to $|p_\downarrow\rangle = |5^2P_{3/2}, F=2, m_F=0\rangle$. We choose control field to be σ_+ polarized, which ensures that coupling to any Rydberg s -states from $|p_\uparrow\rangle$ is zero because $|p_\uparrow\rangle = \frac{1}{\sqrt{2}} [|m_j = \frac{1}{2}\rangle |m_I = \frac{3}{2}\rangle - |m_j = \frac{3}{2}\rangle |m_I = -\frac{1}{2}\rangle]$. Whereas from $|p_\downarrow\rangle$ we can couple with σ_+ control field to two different s -states (because $|p_\downarrow\rangle = \frac{1}{2} [|m_j = -\frac{3}{2}\rangle |m_I = \frac{3}{2}\rangle + |m_j = -\frac{1}{2}\rangle |m_I = \frac{1}{2}\rangle - |m_j = \frac{1}{2}\rangle |m_I = -\frac{1}{2}\rangle - |m_j = \frac{3}{2}\rangle |m_I = -\frac{3}{2}\rangle]$), from which we single out one (i.e., $|S\rangle$ in Fig. 4) by applying external magnetic field. For $|\delta_- \Delta_\downarrow| \gg \Omega^2$ and $\Omega_\uparrow = \Omega\sqrt{2/3}$ both polaritons have the same group velocity, therefore, the time delay inside the medium is the same. This way the only impact of the interaction on the qubit state is the phase shift for $|\downarrow, \downarrow\rangle$ state, which corresponds to $|\mathcal{E}_+ \mathcal{E}_-\rangle$ photons in our analysis of the phase gate fidelity.

Estimate of the optimal parameters for the phase gate—Based on the estimates of all the detrimental effects, we numerically find optimal parameters δ and Ω for fixed C_6 , g , L and ϕ in case of ^{87}Rb atoms (for which $\gamma/\pi = 6.1 \text{ MHz}$). A resulting fidelity for $|100S\rangle$

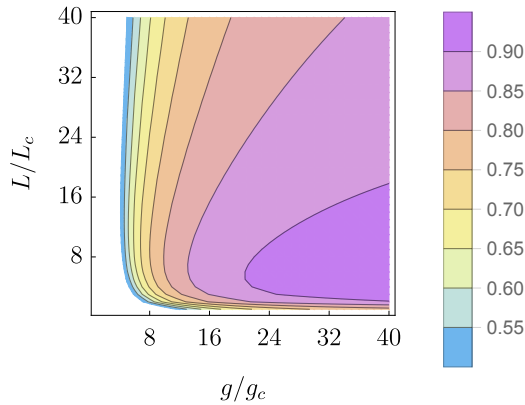


Figure 5. The \sqrt{F} including all presented corrections for $\phi = \pi/2$ as a function of collective coupling g and length of the medium L , with parameters characteristic for experiments presented in Refs [20, 21]: $L_c = 160\mu\text{m}$ and $g_c/2\pi = 4.4\text{GHz}$. All our estimates assume that the corrections are small and a pulse is long, $\sigma_z g^2 / |\Delta|c \gg 1$. Therefore, the estimates are not valid in the regimes where F drops much below 1, therefore, we do not plot fidelity there.

state (for which $\gamma_s/2\pi = 2.3\text{kHz}$) and $\phi = \pi/2$ as a function of g and $L = 2\mathcal{L}$ is presented in Fig. 5. In order to neglect interaction effects for the entering and leaving the medium, as well as to ensure that photons will completely interact with each other, we set $\sigma_z = L/8$. Some of the corrections are overestimated, like scattering to other channels, see Eq. 22, and thus true fidelity can be higher. Presented Fig. 5 shows that the fidelity of a phase gate is not constrained fundamentally. Note that our analysis is a good starting point to find optimal parameters using full two-photon propagation numerics.

Acknowledgments— We thank S. Hofferberth and A.V. Gorshkov for discussions. We acknowledge support by the European Union under the ERC consolidator grant SIRPOL (grant N. 681208). P.B. acknowledges support by by ARL CDQI, ARO MURI, AFOSR, NSF PFC at JQI, DoE ASCR Quantum Testbed Pathfinder Program (award No. DE-SC0019040), DoE BES QIS program (award No. DE-SC0019449), and NSF PFCQC program.

- [1] M. A. Nielsen and I. L. Chuang, *Quantum computation and quantum information* (2000).
- [2] Q. A. Turchette, C. J. Hood, W. Lange, H. Mabuchi and H. J. Kimble, *Measurement of conditional phase shifts for quantum logic*, Phys. Rev. Lett., **75**, 4710–4713 (1995).
- [3] I. Fushman, D. Englund, A. Faraon, N. Stoltz, P. Petroff and J. Vuckovic, *Controlled phase shifts with a single quantum dot.*, Science, **320**, 769–72 (2008).
- [4] V. Parigi, E. Bimbar, J. Stanojevic, A. J. Hilliard, F. Nogrette, R. Tualle-Broui, A. Ourjoumtsev and P. Grangier, *Observation and Measurement of Interaction-Induced Dispersive Optical Nonlinearities in an Ensemble of Cold Rydberg Atoms*, Phys. Rev. Lett., **109**, 233602 (2012).

- [5] J. Volz, M. Scheucher, C. Junge and A. Rauschenbeutel, *Nonlinear π phase shift for single fibre-guided photons interacting with a single resonator-enhanced atom*, Nat Phot., **8**, 965–970 (2014).
- [6] A. Reiserer, N. Kalb, G. Rempe and S. Ritter, *A quantum gate between a flying optical photon and a single trapped atom.*, Nature, **508**, 237–40 (2014).
- [7] M. Fleischhauer, *Electromagnetically induced transparency: Optics in coherent media*, Rev. Mod. Phys., **77**, 633–673 (2005).
- [8] H.-Y. Lo, Y.-C. Chen, P.-C. Su, H.-C. Chen, J.-X. Chen, Y.-C. Chen, I. a. Yu and Y.-F. Chen, *Electromagnetically-induced-transparency-based cross-phase-modulation at attojoule levels*, Phys. Rev. A, **83**, 041804 (2011).
- [9] B. W. Shiau, M. C. Wu, C. C. Lin and Y. C. Chen, *Low-light-level cross-phase modulation with double slow light pulses*, Phys. Rev. Lett., **106**, 193006 (2011).
- [10] A. Feizpour, M. Hallaji, G. Dmochowski and A. M. Steinberg, *Observation of the nonlinear phase shift due to single post-selected photons*, Nat. Phys., **11**, 905–909 (2015).
- [11] K. Nemoto and W. J. Munro, *Nearly deterministic linear optical controlled-NOT gate*, Phys. Rev. Lett., **93**, 250502 (2004).
- [12] A. K. Mohapatra, T. R. Jackson and C. S. Adams, *Coherent Optical Detection of Highly Excited Rydberg States Using Electromagnetically Induced Transparency*, Phys. Rev. Lett., **98**, 113003 (2007).
- [13] J. D. Pritchard, D. Maxwell, A. Gauguier, K. Weatherill, M. Jones and C. Adams, *Cooperative Atom-Light Interaction in a Blockaded Rydberg Ensemble*, Phys. Rev. Lett., **105**, 193603 (2010).
- [14] A. K. Mohapatra, M. G. Bason, B. Butscher, K. J. Weatherill and C. S. Adams, *A giant electro-optic effect using polarizable dark states*, Nat. Phys., **4**, 890–894 (2008).
- [15] T. Peyronel, O. Firstenberg, Q.-Y. Liang, S. Hofferberth, A. V. Gorshkov, T. Pohl, M. D. Lukin and V. Vuletić, *Quantum nonlinear optics with single photons enabled by strongly interacting atoms.*, Nature, **488**, 57–60 (2012).
- [16] Y. O. Dudin and A. Kuzmich, *Strongly interacting Rydberg excitations of a cold atomic gas.*, Science, **336**, 887–9 (2012).
- [17] Y. O. Dudin, F. Bariani and a. Kuzmich, *Emergence of Spatial Spin-Wave Correlations in a Cold Atomic Gas*, Phys. Rev. Lett., **109**, 133602 (2012).
- [18] D. Maxwell, D. J. Szwer, D. P. Barato, H. Busche, J. D. Pritchard, A. Gauguier, K. J. Weatherill, M. P. A. Jones and C. S. Adams, *Storage and Control of Optical Photons Using Rydberg Polaritons*, Phys. Rev. Lett., **110**, 103001 (2013).
- [19] C. S. Hofmann, G. Günter, H. Schempp, M. Robert-de Saint-Vincent, M. Gärttner, J. Evers, S. Whitlock and M. Weidemüller, *Sub-Poissonian Statistics of Rydberg-Interacting Dark-State Polaritons*, Phys. Rev. Lett., **110**, 203601 (2013).
- [20] O. Firstenberg, T. Peyronel, Q.-Y. Liang, A. V. Gorshkov, M. D. Lukin and V. Vuletić, *Attractive photons in a quantum nonlinear medium.*, Nature, **502**, 71–75 (2013).
- [21] H. Gorniaczyk, C. Tresp, J. Schmidt, H. Fedder and S. Hofferberth, *Single Photon Transistor Mediated by Inter-State Rydberg Interaction*, Phys. Rev. Lett., **113**, 053601 (2014).
- [22] S. Baur, D. Tiarks, G. Rempe and S. Dürr, *Single-Photon Switch based on Rydberg Blockade*, Phys. Lev. Lett., **112**, 073901 (2014).
- [23] D. Tiarks, S. Baur, K. Schneider, S. Dürr and G. Rempe, *Single-Photon Transistor Using a Förster Resonance*, Phys. Rev. Lett., **113**, 053602 (2014).
- [24] C. Tresp, P. Bienias, S. Weber, H. Gorniaczyk, I. Mirgorod-

- skiy, H. P. Büchler and S. Hofferberth, *Dipolar Dephasing of Rydberg D-State Polaritons*, Phys. Rev. Lett., **115**, 083602 (2015).
- [25] H. Gorniaczyk, C. Tresp, P. Bienias, A. Paris-Mandoki, W. Li, I. Mirgorodskiy, H. P. Büchler, I. Lesanovsky and S. Hofferberth, *Enhancement of Rydberg-mediated single-photon nonlinearities by electrically tuned Förster resonances*, Nat. Commun., **7**, 12480 (2016).
- [26] C. Tresp, C. Zimmer, I. Mirgorodskiy, H. Gorniaczyk, A. Paris-Mandoki and S. Hofferberth, *Single-photon absorber based on strongly interacting Rydberg atoms*, PRL, **117**, 223001 (2016).
- [27] D. Tiarks, S. Schmidt, G. Rempe and S. Durr, *Optical phase shift created with a single-photon pulse*, Sci. Adv., **2**, e1600036–e1600036 (2016).
- [28] N. Schine, A. Ryou, A. Gromov, A. Sommer, J. Simon, E. Hamiltonian and L. Gauss, *Synthetic Landau levels for photons*, Nature, **534**, 7609 (2016).
- [29] S. Sevincli, N. Henkel, C. Ates, T. Pohl, S. Sevincli, N. Henkel, C. Ates and T. Pohl, *Nonlocal nonlinear optics in cold rydberg gases*, Phys. Rev. Lett., **107**, 153001 (2011).
- [30] A. V. Gorshkov, J. Otterbach, M. Fleischhauer, T. Pohl and M. D. Lukin, *Photon-Photon Interactions via Rydberg Blockade*, Phys. Rev. Lett., **107**, 133602 (2011).
- [31] D. Petrosyan, J. Otterbach and M. Fleischhauer, *Electromagnetically Induced Transparency with Rydberg Atoms*, Phys. Rev. Lett., **107**, 213601 (2011).
- [32] J. Otterbach, M. Moos, D. Muth and M. Fleischhauer, *Wigner Crystallization of Single Photons in Cold Rydberg Ensembles*, Phys. Rev. Lett., **111**, 113001 (2013).
- [33] A. V. Gorshkov, R. Nath and T. Pohl, *Dissipative Many-body Quantum Optics in Rydberg Media*, Phys. Rev. Lett., **110**, 153601 (2013).
- [34] J. Stanojevic, V. Parigi, E. Bimbard, A. Ourjoumtsev and P. Grangier, *Dispersive optical nonlinearities in a Rydberg electromagnetically-induced-transparency medium*, Phys. Rev. A, **88**, 053845 (2013).
- [35] Y. M. Liu, D. Yan, X. D. Tian, C. L. Cui and J. H. Wu, *Electromagnetically induced transparency with cold Rydberg atoms: Superatom model beyond the weak-probe approximation*, Phys. Rev. A, **89**, 033839 (2014).
- [36] B. He, A. V. Sharypov, J. Sheng, C. Simon and M. Xiao, *Two-Photon Dynamics in Coherent Rydberg Atomic Ensemble*, Phys. Rev. Lett., **112**, 133606 (2014).
- [37] A. Grankin, E. Brion, E. Bimbard, R. Boddeda, I. Usmani, A. Ourjoumtsev and P. Grangier, *Quantum statistics of light transmitted through an intracavity Rydberg medium*, New J. Phys., **16**, 043020 (2014).
- [38] W. Li, D. Viscor, S. Hofferberth and I. Lesanovsky, *Electromagnetically induced transparency in an entangled medium*, Phys. Rev. Lett., **112**, 243601 (2014).
- [39] H. Wu, M.-m. Bian, L.-t. Shen, R.-x. Chen, Z.-b. Yang and S.-b. Zheng, *Electromagnetically induced transparency with controlled van der Waals interaction*, ArXiv:1403.5724, **1** (2014).
- [40] P. Bienias, S. Choi, O. Firstenberg, M. F. Maghrebi, M. Gullans, M. D. Lukin, A. V. Gorshkov and H. P. Büchler, *Scattering resonances and bound states for strongly interacting Rydberg polaritons*, Phys. Rev. A, **90**, 053804 (2014).
- [41] A. Sommer, H. P. Büchler and J. Simon, *Quantum Crystals and Laughlin Droplets of Cavity Rydberg Polaritons*, ArXiv:1506.00341 (2015).
- [42] A. Grankin, E. Brion, E. Bimbard, R. Boddeda, I. Usmani, A. Ourjoumtsev and P. Grangier, *Quantum-optical nonlinearities induced by Rydberg-Rydberg interactions: A perturbative approach*, Phys. Rev. A, **92**, 043841 (2015).
- [43] G. W. Lin, Y. H. Qi, X. M. Lin, Y. P. Niu and S. Q. Gong, *Strong photon blockade with intracavity electromagnetically induced transparency in a blockaded Rydberg ensemble*, Phys. Rev. A, **92**, 043842 (2015).
- [44] M. Moos, M. Höning, R. Unanyan and M. Fleischhauer, *Many-body physics of Rydberg dark-state polaritons in the strongly interacting regime*, Phys. Rev. A, **92**, 053846 (2015).
- [45] M. F. Maghrebi, N. Y. Yao, M. Hafezi, T. Pohl, O. Firstenberg and A. V. Gorshkov, *Fractional quantum Hall states of Rydberg polaritons*, Phys. Rev. A, **91**, 033838 (2015).
- [46] M. F. Maghrebi, M. J. Gullans, P. Bienias, S. Choi, I. Martin, O. Firstenberg, M. D. Lukin, H. P. Büchler and A. V. Gorshkov, *Coulomb bound states of strongly interacting photons*, Phys. Rev. Lett., **115**, 123601 (2015).
- [47] T. Caneva, M. T. Manzoni, T. Shi, J. S. Douglas, J. I. Cirac and D. E. Chang, *Quantum dynamics of propagating photons with strong interactions: a generalized input-output formalism*, New J. Phys., **17**, 113001 (2015).
- [48] T. Shi, D. E. Chang and J. I. Cirac, *Multiphoton-scattering theory and generalized master equations*, Phys. Rev. A, **92**, 053834 (2015).
- [49] K. Jachymski, P. Bienias and H. P. Büchler, *Three-body interaction of Rydberg slow light polaritons*, Phys. Rev. Lett., **117**, 053601 (2016).
- [50] M. J. Gullans, J. D. Thompson, Y. Wang, Q.-Y. Liang, V. Vuletic, M. D. Lukin, A. V. Gorshkov, V. Vuletic, M. D. Lukin and A. V. Gorshkov, *Effective Field Theory for Rydberg Polaritons*, Phys. Rev. Lett., **117**, 113601 (2016).
- [51] C. R. Murray, A. V. Gorshkov and T. Pohl, *Many-body decoherence dynamics and optimised operation of a single-photon switch*, New J. Phys., **18**, 17 (2016).
- [52] E. Zeuthen, M. J. Gullans, M. F. Maghrebi and A. V. Gorshkov, *Correlated photon dynamics in dissipative Rydberg media*, ArXiv:1608.06068 (2016).
- [53] W. Li and I. Lesanovsky, *Coherence in a cold-atom photon switch*, Phys. Rev. A, **92**, 043828 (2015).
- [54] C. R. Murray and T. Pohl, *Coherent photon manipulation in interacting atomic ensembles*, Arxiv:1702.03763 (2017).
- [55] P. Bienias and H. P. Büchler, *Quantum theory of Kerr nonlinearity with Rydberg slow light polaritons*, New J. Phys., **18**, 123026 (2016).
- [56] I. Friedler, D. Petrosyan, M. Fleischhauer and G. Kurizki, *Long-range interactions and entanglement of slow single-photon pulses*, Phys. Rev. A, **72**, 043803 (2005).
- [57] D. Paredes-Barato and C. S. Adams, *All-optical quantum information processing using Rydberg gates*, Phys. Rev. Lett., **112**, 040501 (2014).
- [58] M. Khazali, K. Heshami and C. Simon, *Photon-photon gate via the interaction between two collective Rydberg excitations*, PRA, **91**, 030301(R) (2015).
- [59] J. Shapiro, *Single-photon Kerr nonlinearities do not help quantum computation*, Phys. Rev. A, **73**, 062305 (2006).
- [60] J. H. Shapiro and M. Razavi, *Continuous-time cross-phase modulation and quantum computation*, New J. Phys., **9**, 16–16 (2007).
- [61] J. Gea-Banacloche, *Impossibility of large phase shifts via the giant Kerr effect with single-photon wave packets*, Phys. Rev. A, **81**, 043823 (2010).
- [62] M. Mašalas and M. Fleischhauer, *Scattering of dark-state polaritons in optical lattices and quantum phase gate for photons*, Phys. Rev. A, **69**, 061801 (2004).
- [63] A. André, M. Bajcsy, A. Zibrov and M. Lukin, *Nonlinear Optics with Stationary Pulses of Light*, Phys. Rev. Lett., **94**, 063902 (2005).
- [64] E. Shahmoon, G. Kurizki, M. Fleischhauer and D. Pet-

- rosyan, *Strongly interacting photons in hollow-core waveguides*, Phys. Rev. A, **83**, 33806 (2011).
- [65] K. Marzlin, Z. Wang, S. Moiseev and B. Sanders, *Uniform cross-phase modulation for nonclassical radiation pulses*, JOSA B, **27**, 36–45 (2010).
- [66] B. He and A. Scherer, *Continuous-mode effects and photon-photon phase gate performance*, Phys. Rev. A, **85**, 033814 (2012).
- [67] See *Supplementary Material for detailed derivation*.
- [68] D. Tiarks, S. Schmidt-Eberle, T. Stolz, G. Rempe and S. Dürr, *A photonphoton quantum gate based on Rydberg interactions*, Nat. Phys., **15**, 124–126 (2019).
- [69] J. D. Thompson, T. L. Nicholson, Q. Y. Liang, S. H. Cantu, A. V. Venkatramani, S. Choi, I. A. Fedorov, D. Viscor, T. Pohl, M. D. Lukin and V. Vuletic, *Symmetry-protected collisions between strongly interacting photons*, Nature, **542**, 206–209 (2017).
- [70] H. Busche, P. Huillery, S. W. Ball, T. Ilieva, M. P. Jones and C. S. Adams, *Contactless nonlinear optics mediated by long-range Rydberg interactions*, Nat. Phys., **13**, 655–658 (2017).
- [71] Y.-F. Hsiao, P.-J. Tsai, H.-S. Chen, S.-X. Lin, C.-C. Hung, C.-H. Lee, Y.-H. Chen, Y.-F. Chen, I. A. Yu and Y.-C. Chen, *Highly efficient coherent optical memory based on electromagnetically induced transparency*, Phys. Rev. Lett., **120**, 183602 (2016).
- [72] A. Gorshkov, A. André, M. Lukin and A. Sørensen, *Photon storage in Λ -type optically dense atomic media. II. Free-space model*, Phys. Rev. A, **76**, 1–25 (2007).
- [73] A. Asenjo-Garcia, M. Moreno-Cardoner, A. Albrecht, H. J. Kimble and D. E. Chang, *Exponential improvement in photon storage fidelities using subradiance and "selective radiance" in atomic arrays*, Phys. Rev. X, **7**, 031024 (2017).
- [74] P. Bienias, *Few-body quantum physics with strongly interacting Rydberg polaritons*, Eur. Phys. J. ST, **225**, 2957 (2016).
- [75] A. Gorshkov, J. Otterbach, M. Fleischhauer, T. Pohl and M. Lukin, *Photon-Photon Interactions via Rydberg Blockade*, Phys. Rev. Lett., **107**, 1–4 (2011).
- [76] B. He, A. MacRae, Y. Han, A. I. Lvovsky and C. Simon, *Transverse multimode effects on the performance of photon-photon gates*, Phys. Rev. A, **83**, 022312 (2011).
- [77] S. Lloyd, *Almost any Quantum Gate is universal*, Phys. Rev. Lett., **75**, 346 (1995).
- [78] A. Rauschenbeutel, G. Nogues, S. Osnaghi, P. Bertet, M. Brune, J. Raimond and S. Haroche, *Coherent Operation of a Tunable Quantum Phase Gate in Cavity QED*, Phys. Rev. Lett., **83**, 5166–5169 (1999).

Appendix A. Corrections due to inhomogeneous distribution of atoms.

Analogously to [55] we can include a shape of atomic distribution in the solution of the two-body counterpropagating problem. In this section, we will use the notation from [55], i.e., $\beta(x)$ describes the amplitude of the polariton to be in a photonic state and is related to the slow light velocity $v_g = c\beta(x)^2$, while $n(x) = 1 - \beta(x)^2$ is the probability for the polariton to be in the Rydberg state. These quantities are determined by the atomic density $n_{\text{at}}(x)$ via $\beta(x) = \Omega / \sqrt{\Omega^2 + g_0^2 n_{\text{at}}(x)}$ with g_0 the single atom coupling. Then, the solution of two-body problem

$$\phi^{\text{out}}(x, y, t) = e^{-i\varphi(x, y)} \phi^{\text{in}}(x - ct', y + ct') \quad (\text{A.1})$$

where $t' = t - \Delta t$ accounts for the delay of the polaritons inside the medium with $\Delta t = \int_{-\infty}^{\infty} dy (1/\beta(y)^2 - 1) / c$. The phase factor φ describes the correlations built up between the photons during the propagation through the medium and takes the form

$$\varphi(z, z', t) = \frac{1}{\hbar c} \int_{z-ct}^z dw \tilde{n}(w) \tilde{n}(z + z' - w) \tilde{V}(z + z' - w, w) \quad (\text{A.2})$$

where $\tilde{n}(z) = n(\zeta(z))$, $\tilde{V}(z, w) = V(\zeta(z) - \zeta(w))$ with the coordinate transformation taking the form $z = \zeta^{-1}(x) = \int_0^x dy (1/\beta(y)^2)$. For large t and z this integral is equivalent to the integral from $-\infty$ to ∞ . For Gaussian distribution of atoms much longer than the blockade radius, $\mathcal{L} \gg \xi$, the phase factor φ simplifies to

$$\varphi(z, z') = \frac{1}{\hbar c} \int dw \tilde{n} \left(\frac{z + z'}{2} \right)^2 V(\zeta(z + z' - w) - \zeta(w)) \quad (\text{A.3})$$

and can be furthermore transformed using $u = \frac{z+z'}{2}$ and $y = \zeta(u)$,

$$\varphi(z, z') = \frac{1}{\hbar c} \tilde{n}(u)^2 \int dw V(\partial_u \zeta(u) 2w) \quad (\text{A.4})$$

$$\varphi(z, z') = \frac{1}{\hbar c} \tilde{n}(u)^2 \int dw V(\beta(y)^2 2w) \quad (\text{A.5})$$

The integral can be calculated analytically, leading to

$$\varphi(z, z') = \frac{1}{\hbar c} n(y)^2 \frac{2\pi}{3} \frac{\xi}{2\beta(y)^2} \frac{2\Omega^2}{\Delta} \quad (\text{A.6})$$

For $g \gg \Omega$ and compressed pulses shorter than the cloud's length, we can set $n(y) = 1$, leading to

$$\varphi(z, z') \approx \frac{1}{\hbar c} \frac{2\pi}{3} \frac{g_0^2 n_{\text{at}}(y)}{\Omega^2} \frac{\xi}{2} \frac{2\Omega^2}{\Delta} \quad (\text{A.7})$$

For small y , using that $u = \zeta^{-1}(y) = \frac{g_0^2 n_0}{\Omega^2} \frac{\sqrt{\pi}}{2} \mathcal{L} \text{Erf}(y/\mathcal{L}) + y \approx \left(1 + \frac{g_0^2 n_0}{\Omega^2}\right) y$, we can write

$$y = \zeta(u) \approx \left(1 + \frac{g_0^2 n_0}{\Omega^2}\right)^{-1} u, \quad (\text{A.8})$$

which gives

$$\varphi\left(u = \frac{z + z'}{2}\right) = \varphi_0 \exp\left[-\left(\frac{uv_g}{c\mathcal{L}}\right)^2\right], \quad (\text{A.9})$$

from which,

$$\beta_{\text{at}} e^{i\phi_0 + i\Delta\phi_{\text{at}}} = \lim_{t \rightarrow \infty} \langle \mathcal{E}\mathcal{E} | \mathcal{E}\mathcal{E}^V \rangle = \lim_{t \rightarrow \infty} \int dz dz' e^{i\phi_0} \mathcal{N}^2 e^{-(z-z_0-ct)^2/s_z^2} e^{-(z'+z_0+ct)^2/s_z^2} \exp\left[i\phi_0 \left(e^{-(\frac{uv_g}{c\mathcal{L}})^2} - 1\right)\right],$$

where as initial conditions we have chosen two Gaussian wavepackets centered at positions $\pm z_0$ with width s_z and normalization factor \mathcal{N} . This integral can be calculated analytically for $s_z/c \ll \mathcal{L}/v_g$, leading to

$$\beta_{\text{at}} e^{i\Delta\phi_{\text{at}}} = \left(1 + \frac{i\phi_0 v_g^2 s_z^2}{2c^2 \mathcal{L}^2}\right)^{-1/2}. \quad (\text{A.10})$$

Expanding it in small parameter $\frac{s_z v_g}{c\mathcal{L}}$ we get

$$\beta_{\text{at}} = 1 - \frac{3}{2}\phi_0^2 \left(\frac{s_z v_g}{2c\mathcal{L}}\right)^4, \quad (\text{A.11})$$

$$\Delta\phi_{\text{at}} = -\phi_0 \left(\frac{s_z v_g}{2c\mathcal{L}}\right)^2, \quad (\text{A.12})$$

which corresponds to the expressions from the main text because $s_z = \sigma_z c/v_g$.

Appendix B. Transversal size effects

The propagation of photons within paraxial approximation is described by the Hamiltonian (analogous to Eq. 4) given by

$$H_{\pm} = \hbar \int d\mathbf{z} \begin{pmatrix} \hat{\mathcal{E}}_{\pm}(\mathbf{z}) \\ \hat{\mathcal{P}}_{\pm}(\mathbf{z}) \\ \hat{\mathcal{S}}_{\pm}(\mathbf{z}) \end{pmatrix}^{\dagger} \begin{pmatrix} \mp ic\partial_z - \frac{c}{2k_p}\nabla_{\perp}^2 & g_0\sqrt{n(\mathbf{z})} & 0 \\ g_0\sqrt{n(\mathbf{z})} & \Delta & \Omega \\ 0 & \Omega & 0 \end{pmatrix} \begin{pmatrix} \hat{\mathcal{E}}_{\pm}(\mathbf{z}) \\ \hat{\mathcal{P}}_{\pm}(\mathbf{z}) \\ \hat{\mathcal{S}}_{\pm}(\mathbf{z}) \end{pmatrix}. \quad (\text{B.1})$$

where k_p is the carrier frequency of the probe photons. We are interested in an estimate of leading corrections to the fidelity, thus we neglect transversal corrections to the dispersion relation of photons. In addition, we consider atomic distribution broader than the extend of relevant photonic modes, leading to

$$H_{\pm} = \hbar \int d\mathbf{z} \begin{pmatrix} \hat{\mathcal{E}}_{\pm}(\mathbf{z}) \\ \hat{\mathcal{P}}_{\pm}(\mathbf{z}) \\ \hat{\mathcal{S}}_{\pm}(\mathbf{z}) \end{pmatrix}^{\dagger} \begin{pmatrix} \mp ic\partial_z & g_0\sqrt{n_{\text{at}}} & 0 \\ g_0\sqrt{n_{\text{at}}} & \Delta & \Omega \\ 0 & \Omega & 0 \end{pmatrix} \begin{pmatrix} \hat{\mathcal{E}}_{\pm}(\mathbf{z}) \\ \hat{\mathcal{P}}_{\pm}(\mathbf{z}) \\ \hat{\mathcal{S}}_{\pm}(\mathbf{z}) \end{pmatrix}. \quad (\text{B.2})$$

Then, the solution of interacting two-body problem can be derived analogously to Eq. 11 leading to

$$\psi_{k_D}^{ss}(r, \mathbf{R}_+, \mathbf{R}_-) = \frac{1}{1 - \bar{\chi}V(\mathbf{r})} u_{00}(\mathbf{R}_+) u_{00}(\mathbf{R}_-) e^{ik_D r} \exp \left[-i \frac{\alpha_D}{\hbar} \int_{-\infty}^r dz V^{\text{eff}}(|\mathbf{R}_+ - \mathbf{R}_-|, z) \right] \quad (\text{B.3})$$

where $\mathbf{r} = \{r, \mathbf{R} = \mathbf{R}_+ - \mathbf{R}_-\}$ with r being the longitudinal component of relative distance, and \mathbf{R}_{\pm} are transverse components of the \mathbf{z}_{\pm} (\mathbf{z}_{\pm} corresponds to \mathbf{z} in Eq. B.2 for two directions of the propagation). u_{00} is the lowest Laguerre-Gauss mode describing transverse shape of the incoming photons (in the main text u_{00} is denoted by u). This solution in the limit of $r \rightarrow \infty$ leads to the expression for β_{tr} from the main text.

Appendix C. Summary of the corrections to the fidelity

β_j	estimate
β_{γ}	$e^{-2\eta}$, with $\eta = \phi \frac{5}{6} \frac{\gamma}{\delta}$
$ \beta_{\text{sc}} $	$1 - \phi^2 \frac{\Omega^2}{ \Delta ^2} \frac{ \Delta ^2 + g^2}{4g^2}$,
β_{wp}	$P_+ P_- \exp \left[-\frac{49}{2} \phi^2 \left(\frac{\sigma \Delta }{12\Omega^2} \right)^2 \right]$, where $P_{\pm} = \exp \left[-2 \frac{Lg^2}{\delta c} \left(\frac{\delta\sigma}{\Omega^2} \right)^2 \frac{\gamma}{\delta} \right]$
β_{at}	$1 - \frac{3}{2} \phi^2 \left(\frac{\sigma_z}{2c\mathcal{L}} \right)^4$.
β_{tr}	$\mathcal{F}(w_0/\xi)$
β_{Ry}	$e^{-4\gamma_s L/v_g}$

Table C1. Summarizing table of analyzed contributions to the fidelity.

In the TAB. C1 we sum-up all the estimates for the corrections to the phase gate fidelity F , given by Eq. 3. In order to generate results presented in Fig. 5 and Fig. D1, we maximize the value of \sqrt{F} for fixed w_0, ϕ, C_6 in function of g, L , by finding optimal detuning δ . Then, the value of Rabi frequency Ω is fixed by the constraint on ϕ .

Appendix D. Results for alternative definition of fidelity: conditional-fidelity

In Fig. D1 we show the conditional-fidelity $\sqrt{F_{\text{cond}}}$ which contains all presented corrections except single body losses (i.e. we set $P_{\pm} = 1$ and $\beta_{\text{Ry}} = 0$) for parameters as in Fig. 5.

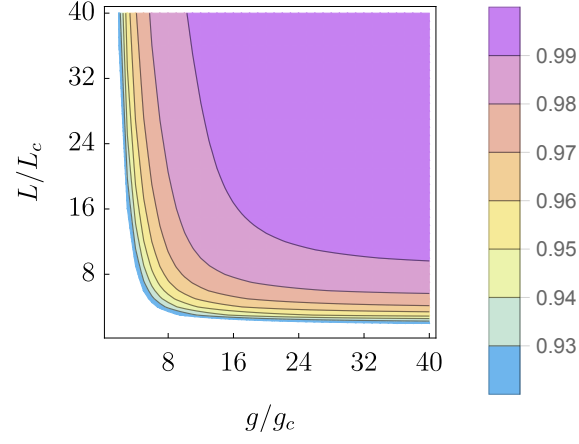


Figure D1. The $\sqrt{F_{\text{cond}}}$ which contains all presented corrections except single body losses (i.e. we set $P_{\pm} = 1$ and $\beta_{\text{Ry}} = 1$) for parameters as in Fig. 5.